Molecular cation NHe^{2+}

G. P. Lafyatis
The Department of Physics, The Ohio State University, Columbus, Ohio 43210

K. Kirby and A. Dalgarno
The Harvard-Smithsonian Center for Astrophysics, Cambridge, Massachusetts 02138

(Received 25 November 1992)

The potential-energy curves of the low-lying $^2\Sigma^+$ and $^2\Pi$ states of the cation NHe^{2+} are calculated and it is shown that the lowest state of each symmetry has a potential well inside a repulsive Coulomb barrier that contains several long-lived vibrational levels. Estimates are made of the cross sections of the charge-transfer processes $N^{2+}+He \rightarrow N^+ + He^+$ which occur through transitions at avoided crossings of the molecular states.

PACS number(s): 34.20.−b, 34.70.+e

I. INTRODUCTION

Doubly charged molecular ions containing helium and transition metals were detected experimentally by Tsong and Kinkus [1] and studied theoretically by Hotokka *et al.* [2]. The simple dication CHe^{2+} has been studied theoretically by Harrison *et al.* [3], Cooper and Wilson [4], Koch *et al.* [5], and Koch, Frenking, and Luke [6]. Here we explore the structure of the low-lying states of the dication NHe^{2+}. These same states control the charge transfer in collisions of N^{2+} and He and we carry out Landau-Zener calculations of the cross sections for the process

$$N^{2+}+He \rightarrow N^+ + He^+ , \quad (1)$$

for which laboratory measurements exist [7–11].

II. ELECTRONIC STATES OF NHe^{2+}

The entrance channels for the charge-transfer reaction (1) are electronic states of the molecular ion NHe^{2+} of $^2\Sigma^+$ and $^2\Pi$ symmetries separating at large internuclear distances to the doubly charged $N^{2+}(2p,{}^2P^o)$ ion and a neutral helium atom $He(1s^2,{}^1S)$. At large separations, the potential energy tends to the polarization attraction $-2\alpha R^{-4}$ where α is the polarizability of He. Lower-lying channels separate into pairs of singly charged ions N^+ and He^+ with potential energy dominated by the $1/R$ Coulomb repulsion. Because of the Coulomb repulsion, avoided crossings of adiabatic potential-energy curves of states of the same symmetry occur. To explore their influence on the structure of the cation, we have used a configuration-interaction method to calculate the electronic eigenfunctions and potential energies of several of the low-lying $^2\Sigma^+$ and $^2\Pi$ states of NHe^{2+}.

The process of charge exchange often involves the interaction of several states of the same symmetry but different character, which is manifested in the adiabatic picture as avoided crossings such as those we see in the NHe^{2+} cation. The internuclear distances of the avoided crossings are critical parameters in the calculation of the charge-transfer cross sections. In a zero-order model, these distances R_x are determined by the asymptotic energy splitting ΔE of the ionic and neutral channels such that $R_x \sim \Delta E^{-1}$. Therefore it is necessary to describe several states of the same symmetry and their respective atomic or ionic asymptotes in an unbiased way. Electronic wave functions were explicitly constructed to minimize the error in the energy differences of the four relevant asymptotes listed in Table I.

To obtain a set of molecular orbitals appropriate for several states of both $^2\Sigma^+$ and $^2\Pi$ symmetries, a state-averaged multiconfiguration self-consistent-field (MCSCF) calculation was performed at each internuclear distance using the three lowest roots of $^2\Pi$ symmetry. The 1σ orbital (essentially, the $1s$ orbital of N) was kept doubly occupied and the valence orbitals determined in the MCSCF procedure consisted of the 2σ, 3σ, 4σ, and 1π orbitals. The orbitals were expanded in the set of

TABLE I. Asymptotic energy splittings, ΔE (obtained by subtraction of energies at $R=\infty$ listed in Table III).

		ΔE (eV)	
	Correlating molecular state	Calculation	Experiment[a]
$N^+(2p^2,{}^3P)+He^+({}^2S)$	$1\,{}^2\Pi$		
$N^+(2p^2,{}^1D)+He^+({}^2S)$	$2\,{}^2\Pi, 1\,{}^2\Sigma^+$	1.96	1.90
$N^+(2p^2,{}^1S)+He^+({}^2S)$	$3\,{}^2\Sigma^+$	4.17	4.05
$N^{2+}(2p,{}^2P^o)+He({}^1S)$	$3\,{}^2\Pi, 2\,{}^2\Sigma^+$	4.96	5.02

[a]Reference [13].

Slater-type functions listed in Table II. The basis set was taken from tables of Clementi and Roetti [12], with additional functions included to describe polarization and correlation effects. With the core and valence orbitals determined, the remainder of the basis allowed for 18σ, 12π, and 5δ virtual (unoccupied) orbitals.

Configuration-interaction wave functions for $^2\Pi$ and $^2\Sigma^+$ symmetries were constructed from a reference space consisting of all arrangements of the five valence electrons in the valence orbitals allowed by symmetry considerations and then including all single and double excitations from this reference space into the virtual orbitals. The $^2\Sigma^+$ calculation included 14 435 configuration state functions and the $^2\Pi$ included 23 169. Calculations were carried out over a range of internuclear separations from $1.5a_0$ to $20a_0$. The potential curves of the lowest three states are given numerically in Table III and shown graphically in Figs. 1 and 2. Figures 1 and 2 include also the potential-energy curves of two higher states of each symmetry.

The computed energy splittings at $R=20a_0$ are listed in Table I after subtraction of the Coulomb repulsion contribution of 1.36 eV in the states separating to $N^+ + He^+$. They agree well with the experimental splittings [13] with a difference of only 0.06 eV for the second and third roots and 0.12 eV for the fourth. The agreement is more impressive because the states separating to $N^{2+}+He$ have a different source of correlation error than the ion-ion states.

Although not shown in Fig. 1, the $^2\Sigma^+$ curve which separates to the $N^+(2p^2,{}^1S)+He^+$ limit has an avoided crossing near $30a_0$ with the state that separates to $N^{2+}(2p,{}^2P^o)+He$. Because the avoided crossing is located at a large internuclear distance, its effect on the structure of the electronic states at smaller distances and its influence on the charge-transfer process are slight and it is convenient to assume that the curves *do* cross. Accordingly we use the numerical labels for the states that are consistent with their order at small separations and designate the state separating to $N^{2+}(2p,{}^2P^o)+He$ as $2\,{}^2\Sigma^+$.

The Coulomb repulsion gives rise to the avoided crossing near $9a_0$ of the $1\,{}^2\Sigma^+$ and $2\,{}^2\Sigma^+$ curves. There is a second avoided crossing of the two states near $2.4a_0$ which significantly modifies their potential-energy curves. It occurs because the $2\,{}^2\Sigma^+$ state has as its dominant configuration $1\sigma^2 2\sigma^2 3\sigma^2 4\sigma$, whereas the lowest state of the united atom limit F^{2+} corresponds to $1\sigma^2 2\sigma^2 3\sigma 1\pi^2$.

The $3\,{}^2\Sigma^+$ state separates to $N^+(2p^2,{}^1S)+He^+$ after crossing the $2\,{}^2\Sigma^+$ state at a large separation. The $4\,{}^2\Sigma^+$ and $5\,{}^2\Sigma^+$ curves lie higher in energy; their end products are, respectively, the limits $N^+(2s2p^3,{}^3P)+He^+$ and $N^{2+}(2s2p^2,{}^2D)+He$. The avoided crossing at $6a_0$ arises from the Coulomb repulsion of the lower state.

The structure of the $^2\Pi$ potential curves differs from that of the $^2\Sigma^+$ curves because there is no $^2\Pi$ curve separating to $N^+(2p^2,{}^1S)+He$ like the $2\,{}^2\Sigma^+$ curve and

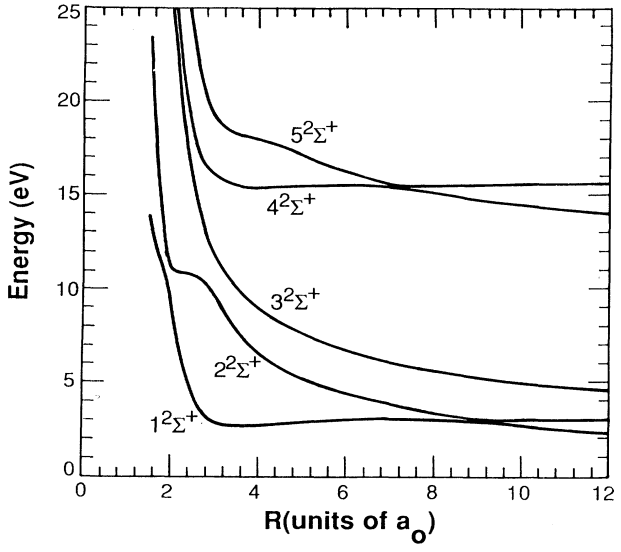

FIG. 1. $^2\Sigma^+$ potential-energy surfaces of NHe^{2+}. $E=0$ corresponds to the $N^+(^1D)+He^+$ limit.

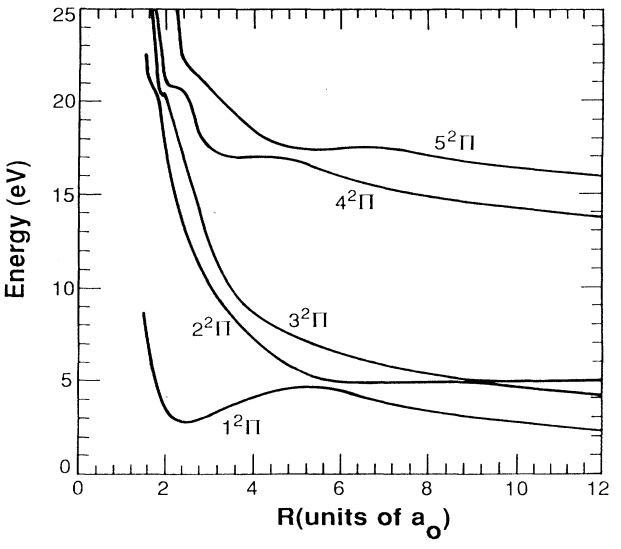

FIG. 2. $^2\Pi$ potential-energy surfaces of NHe^{2+}. $E=0$ corresponds to the $N^+(^3P)+He^+$ limit.

TABLE II. Slater-type basis set.

	n	l[a]	ζ
N	1	0	10.6143, 6.423 21
	2	0	6.156 03, 2.534 45, 1.791 67
	2	1	8.001 93, 3.385 77, 1.975 95, 1.478 88, 1.0
	3	2	4.0, 2.1679
	4	3	3.3
He	1	0	3.3, 1.52
	2	0	3.3, 1.52
	2	1	4.1, 2.4, 1.6
	3	2	4.1, 1.3

[a]All allowed m values from $m=0$ to $m=l$ (for $l\leq 2$) are included.

TABLE III. Potential energies of the low-lying $^2\Sigma^+$ and $^2\Pi$ states of NHe^{+2} (hartrees).

R	$1\,^2\Sigma^+$	$2\,^2\Sigma^+$	$3\,^2\Sigma^+$	$1\,^2\Pi$	$2\,^2\Pi$	$3\,^2\Pi$
1.50	−55.404 86	−55.053 20	−54.723 56	−55.662 88	−55.158 27	−54.880 80
1.75	−55.502 43	−55.380 08	−54.852 04	−55.796 99	−55.232 16	−55.165 84
2.00	−55.589 70	−55.512 89	−55.029 02	−55.855 52	−55.341 78	−55.236 00
2.25	−55.698 65	−55.518 39	−55.197 14	−55.879 50	−55.447 76	−55.308 84
2.50	−55.761 16	−55.520 96	−55.333 19	−55.885 48	−55.517 36	−55.380 14
3.00	−55.810 96	−55.563 50	−55.482 45	−55.873 74	−55.609 56	−55.525 21
3.50	−55.819 69	−55.628 55	−55.545 52	−55.853 93	−55.674 98	−55.617 99
3.75	−55.819 03	−55.653 54	−55.566 68	−55.844 86	−55.701 40	−55.646 38
4.00	−55.817 31	−55.673 40	−55.584 42	−55.837 04	−55.723 98	−55.667 67
4.50	−55.813 39	−55.702 58	−55.612 92	−55.825 44	−55.759 02	−55.698 08
4.75	−55.811 73	−55.713 76	−55.624 63	−55.821 51	−55.772 50	−55.709 72
5.00	−55.810 36	−55.723 46	−55.635 07	−55.818 74	−55.783 84	−55.719 86
5.25	−55.809 26	−55.732 07	−55.644 46	−55.817 19	−55.793 20	−55.728 88
5.50	−55.808 39	−55.739 82	−55.652 97	−55.817 32	−55.800 27	−55.737 01
5.75	−55.807 72	−55.746 90	−55.660 73	−55.819 94	−55.804 33	−55.744 42
7.00	−55.806 00	−55.775 15	−55.691 28	−55.845 98	−55.805 77	−55.773 78
8.00	−55.805 49	−55.791 88	−55.708 96	−55.863 11	−55.805 26	−55.790 97
8.50	−55.805 34	−55.798 87	−55.716 26	−55.870 25	−55.805 10	−55.798 11
8.70	−55.805 29	−55.801 45	−55.718 95	−55.872 88	−55.805 05	−55.800 74
9.00	−55.805 28	−55.805 08	−55.722 76	−55.876 62	−55.805 00	−55.804 47
9.50	−55.810 75	−55.805 15	−55.728 58	−55.882 34	−55.810 20	−55.804 90
10.00	−55.815 84	−55.805 09	−55.733 82	−55.887 50	−55.815 36	−55.804 83
15.00	−55.848 46	−55.804 88	−55.767 08	−55.920 44	−55.848 29	−55.804 61
20.00	−55.864 97	−55.804 85	−55.783 73	−55.937 02	−55.864 87	−55.804 57
∞	−55.914 97	−55.804 84	−55.833 73	−55.987 02	−55.914 87	−55.804 56

there is no $^2\Sigma^+$ curve separating to $N^+(2p^2,{}^3P)+He^+$ like the $1\,^2\Pi$ curve; the $^2\Sigma$ curve separating to this latter limit has $^2\Sigma^-$ symmetry.

The $1\,^2\Sigma^+$ and $1\,^2\Pi$ potential-energy curves are repulsive at large distances, but have deep wells at shorter distances inside repulsive barriers. The predicted equilibrium separation of the $1\,^2\Pi$ state is $2.5a_0$; the well depth is 1.86 eV (calculated from the minimum of the well to the top of the barrier), and the barrier height (with respect to the potential energy as $R\rightarrow\infty$) is 4.62 eV. The equilibrium separation of the $1\,^2\Sigma^+$ state is $3.53a_0$, its well depth is 0.39 eV, and the barrier height is 2.98 eV.

The lowest vibrational levels of the $1\,^2\Pi$ and $1\,^2\Sigma^+$ states lie, respectively, 2.8 and 2.6 eV above the dissociation limits, so that all of the vibrational levels can predissociate by tunneling. The low-lying levels are effectively trapped by the high and wide barriers formed by the Coulomb repulsion of the ionic fragments and therefore can be expected to have long lives against predissociation. The $1\,^2\Sigma^+$ state has 10 long-lived vibrational states and the $1\,^2\Pi$ at least 19. The energies E_v and the energy differences $\Delta G_{v+1/2}$ of the lowest ten vibrational levels of angular momentum, $J=1$ for the $1\,^2\Pi$ state and $J=0$ for the $1\,^2\Sigma^+$ state, are presented in Table IV.

TABLE IV. Vibrational energy levels (eV relative to dissociation limit) and differences (cm^{-1}).

$1\,^2\Pi$ $(J=1)$			$1\,^2\Sigma$ $(J=0)$		
v	E_v	$\Delta G_{v+1/2}$	v	E_v	$\Delta G_{v+1/2}$
0	2.833		0	2.626	
1	2.968	1087	1	2.687	499
2	3.098	1051	2	2.744	454
3	3.224	1021	3	2.794	406
4	3.347	991	4	2.838	358
5	3.466	957	5	2.877	309
6	3.580	923	6	2.909	259
7	3.691	890	7	2.935	209
8	3.797	856	8	2.955	160
9	3.897	821	9	2.970	125

III. CHARGE TRANSFER

Estimates of the cross sections for the charge-transfer processes

$$N^{2+}+He\rightarrow N^+(2p^2,{}^1D)+He\ ,$$
$$N^{2+}+He\rightarrow N^+(2p^2,{}^3P)+He\ , \qquad (2)$$

may be readily obtained using the Landau-Zener approximation. The approach of the N^{2+} and He may occur in the $2\,^2\Sigma^+$ and the $3\,^2\Pi$ electronic states of NHe^{2+}. Charge transfer is described by the transition at an avoided crossing of the system from one of these states to a molecular state with an asymptotic limit given by the right-hand side of either of Eqs. (2). For charge transfer leading to a $N^+(2p^2,{}^1D)$ ion important avoided crossings occur between the 2 and 3 states of the Π symmetry (near $9a_0$) and between the 1 and 2 states of the Σ^+ symmetry (near $9a_0$ and $2.4a_0$). For transfer producing a N^+ ion in

the $(2p^2,{}^3P)$ state, there is no avoided crossing of the $^2\Sigma$ states, one being of $^2\Sigma^+$ symmetry and the other of $^2\Sigma^-$. But for the $^2\Pi$ states, the avoided crossing between states 1 and 2 near $5.5a_0$ is important.

In the Landau-Zener approximation, the probability p that a system makes a transition from one adiabatic potential V_i to another V_f as it passes through an avoided crossing at internuclear separation R_x with radial velocity $v(R_x)$ is given by

$$p=\exp(-\omega)\ , \tag{3}$$

where

$$\omega=\frac{\pi^2\Delta E^2(R_x)}{hv(R_x)}\left|\frac{d}{dR}(V_i-V_f)\right|_{R_x}\ , \tag{4}$$

$\Delta E(R_x)$ being the energy separation at the avoided crossing. If E_i is the initial kinetic energy at infinite separation in the entrance channel and μ is the reduced mass, the radial velocity $v(R_x)$ for nuclear rotational quantum number J is given by

$$\tfrac{1}{2}\mu v(R_x)^2=E_i-V_i(R_x)-\frac{J(J+1)}{2\mu R_x^2}\ . \tag{5}$$

The cross section σ is expressed in terms of P_{if}, the probability that a system initially in channel i exits in channel f. The cross section for transition i to f is

$$\sigma_{if}=\frac{\pi g_i}{k_i^2}\sum_{J=0}^{J_{\max}}(2J+1)P_{if}\ , \tag{6}$$

where g_i is the probability the particles approach in electronic state i, $k_i=\mu v_i/\hbar$ is the initial wave number, and $J_{\max}$ is the largest value of J for which the crossing point is energetically accessible.

For approach along the $2\,^2\Sigma^+$ curve, $g_i=\frac{1}{3}$. Charge transfer is described by the system exiting along the $1\,^2\Sigma^+$ curve. The probability of doing so is a sum of the probabilities for the individual suitable paths:

$$\begin{aligned}P_{21}=&2p_1(1-p_1)p_2^2+2p_1(1-p_1)(1-p_2)^2\\&+2p_1^2p_2(1-p_2)+2(1-p_1)^2p_2(1-p_2)\ ,\end{aligned} \tag{7}$$

where p_1 is the probability of a transition at the $9a_0$ avoided crossing and p_2 is the probability at $2.4a_0$. This process yields a N^+ ion in the $(2p^2,{}^1D)$ state.

For approach along the $3\,^2\Pi$ curve, $g_i=\frac{2}{3}$ and there are two possible charge-transfer end products. The total probability for transition to the $N^+(^1D)+He^+$ exit channel is

$$P_{32}=(1-p_3)p_3+p_3p_4^2(1-p_3)+p_3(1-p_4)^2(1-p_3)\ , \tag{8}$$

where p_3 is the probability of crossing at $9a_0$ for the $^2\Pi$ symmetry and p_4 is the probability at $5.5a_0$.

For the $N^+(^3P)+He^+$ products,

$$P_{31}=2p_3p_4(1-p_4)\ . \tag{9}$$

If the transition probability at an avoided crossing is equal to the adiabatic limit of zero, or the diabatic limit of unity, the avoided crossing will *not* lead to charge transfer.

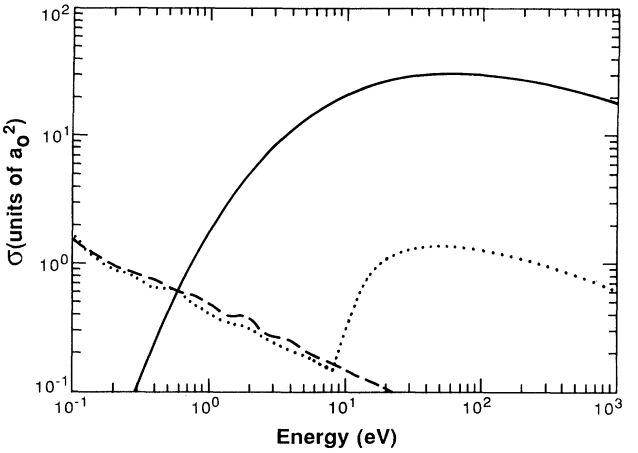

FIG. 3. Partial cross sections by channel and electronic state for producing $N^+(^3P)$ and $N^+(^1D)$ ions. The dotted line ($\cdots$) corresponds to the $^2\Sigma$ channel leading to $N^+(^1D)$; the dashed line ($---$) corresponds to the $^2\Pi$ channel leading to $N^+(^1D)$; and the solid line corresponds to the $^2\Pi$ channel leading to $N^+(^3P)$.

Figure 3 shows our Landau-Zener estimates for charge transfer to $N^+(^1D)$ in the $^2\Sigma^+$ state. At low velocities, the charge transfer occurs predominantly at the outer crossing; at high velocities inner crossing transitions dominate. Figure 3 also shows the charge-transfer cross sections for producing $N^+(^1D)$ and $N^+(^3P)$ in the $^2\Pi$ symmetry. Here charge transfer at low energies occurs most often at the outer crossing and produces $N^+(^1D)$. At high energies, charge transfer via the inner crossing giving $N^+(^3P)$ is predicted to dominate.

Figure 4 compares the total cross sections for charge transfer to $N^+(^1D)$ and $N^+(^3P)$ and their sum, which is the total charge-transfer cross section. The latter has

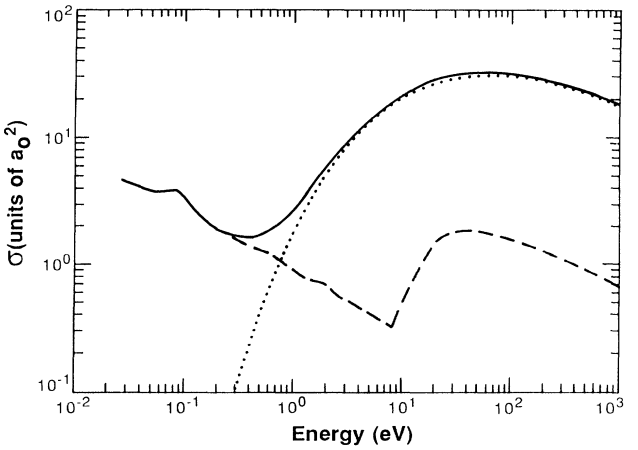

FIG. 4. Charge-transfer cross sections for the production of $N^+(^3P)$ and $N^+(^1D)$ ions. The solid line is the total charge-transfer cross section; the dotted line ($\cdots$) corresponds to the $N^+(^3P)$ channel; and the dashed line ($---$) to the $N^+(^1D)$ channel.

been measured by Hormis, Kamber, and Hasted [8], who found a total charge-transfer cross section of $37a_0^2$ at 450-eV center-of-mass energy, in reasonable agreement with our estimate of $23a_0^2$.

In Fig. 5 we show our estimates of the ratio of the cross section for producing $N^+(^3P)$ to that for $N^+(^1D)$ and record the various experimental results [7–11]. The experiments suggest the basic qualitative trend of our results: $N^+(^1D)$ ions are dominantly produced at low energies, in agreement with an earlier treatment [14], and $N^+(^3P)$ production dominates at high energies. However, there are significant quantitative differences between our theory and the experiments. Although the measurements at high energies are scattered over almost an order of magnitude, the general trend suggests that our results underestimate the probability of producing $N^+(^1D)$ relative to that of making $N^+(^3P)$. For these energies, the reliability of the theory in predicting the cross section for $N^+(^1D)$ production is low. The avoided crossings are passed nearly diabatically and contribute little charge exchange. Because of this, couplings to higher states which are accessible at these energies become *relatively* more important and the Landau-Zener approximation may be inadequate. The agreement between theory and experiment for the charge-transfer process at 450 eV, which leads mostly to $N^+(^3P)$, is consistent with the view that we are underestimating the cross section for producing $N^+(^1D)$ ions.

The disagreement at low energies is unexpected. The essential physics at low energies should be well described in our treatment, the region of small internuclear separations, where the couplings to additional states are large, being inaccessible. The effect of rotational angular coupling may be significant. Further experiments would be instructive.

After these calculations were completed, our attention was drawn to the paper by Nikitin and Reznikov [15] in which Landau-Zener calculations of the cross sections are reported. The empirical potential-energy curves on which they are based agree satisfactorily with our *ab initio* curves at large distances and show diabatic crossings of the $^2\Sigma^+$ states near $8.70a_0$ and of the $^2\Pi$ states near $8.65a_0$ and $5.5a_0$. Because their calculations do not extend below $4a_0$, they did not find the $^2\Sigma^+$ crossing at $2.4a_0$.

The inner crossing makes a significant contribution to the charge transfer into the $N^+(^1D)$ at energies above 10 eV. Below 10 eV, our cross sections for $N^+(^1D)$ production agree closely with those of Nikitin and Reznikov [15]. Our cross sections for $N^+(^3P)$ production have a similar behavior with energy in the limited range over which Nikitin and Reznikov presented cross sections, but because of different assumptions about the coupling strength, differ in magnitude. Thus Nikitin and Reznikov obtained cross sections for $N^+(^3P)$ increasing from 1.0×10^{-16} cm^2 at 4 eV to 3.4×10^{-16} cm^2 at 12 eV, whereas we obtained 2.8×10^{-16} cm^2 at 4 eV increasing to 6.7×10^{-16} cm^2 at 12 eV.

Both sets of calculations yield a cross section ratio for ^3P to ^1D production much greater than the measured ratio [11]. Similar discrepancies occur for collisions of Kr^{2+} in He and Ar^{2+} in He [15].

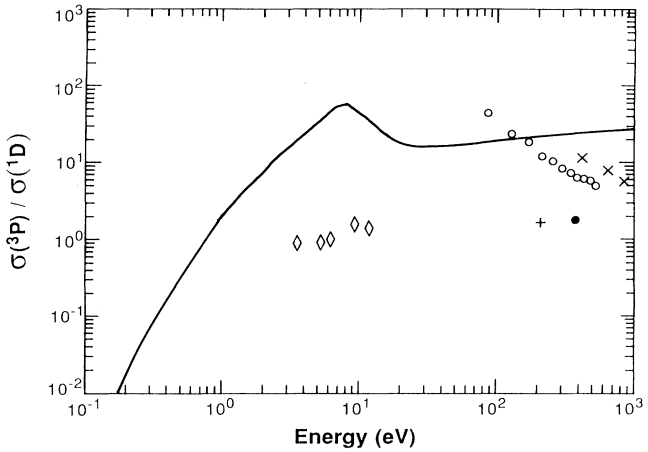

FIG. 5. Ratio of cross sections for $N^+(^3P)$ and $N^+(^1D)$ ions. The solid line represents the present work; experimental measurements are shown as follows: ◇, Ref. [11]; □, Ref. [7]; +, Ref. [8]; ●, Ref. [9]; ×, Ref. [10].

ACKNOWLEDGMENTS

This work was supported by the U.S. Department of Energy, Division of Energy Sciences, Office of Energy Research. G.P.L. acknowledges support from the NSF. We are indebted to Z. Herman for discussions and for bringing Ref. [15] to our attention.

[1] T. T. Tsong and T. J. Kinkus, Phys. Scr. **T4**, 201 (1983).
[2] M. Hotokka, T. Kindstedt, P. Pyykko, and B. O. Roos, Mol. Phys. **52**, 23 (1984).
[3] S. W. Harrison, G. A. Henderson, L. J. Massa, and P. Solomon, Astrophys. J. **189**, 605 (1974).
[4] D. L. Cooper and S. Wilson, Mol. Phys. **44**, 161 (1981).
[5] W. Koch, G. Frenking, J. Gauss, D. Cremer, and J. R. Collins, J. Am. Chem. Soc. **109**, 5917 (1987).
[6] W. Koch, G. Frenking, and B. T. Luke, Chem. Phys. Lett. **139**, 149 (1987).
[7] Y. Sato and J. H. Moore, Phys. Rev. A **19**, 95 (1979).
[8] W. G. Hormis, E. Y. Kamber, and J. B. Hasted, Int. J. Mass Spectrom. Ion Processes **69**, 21 (1986).
[9] S. Sharma, G. L. Awad, J. B. Hasted, and D. Mather, J. Phys. B **12**, L163 (1979).
[10] M. Lennon, R. W. McCullough, and H. B. Gilbody, J. Phys. B **16**, 2191 (1983).
[11] M. Sadilek, J. Vancura, M. Farnik, and Z. Herman, Int. J. Mass Spectrom. Ion. Processes **100**, 197 (1990).
[12] E. Clementi and C. Roetti, At. Data Nucl. Data Tables **14**, 177 (1974).
[13] C. E. Moore, *Atomic Energy Levels*, Natl. Bur. Stand. Ref. Data Ser., Natl. Bur. Stand. (U.S.) Circ. No. 34 (U.S. GPO, Washington, D.C., 1971), Vol. I.
[14] S. E. Butler and A. Dalgarno, Astrophys. J. **241**, 838 (1980).
[15] E. E. Nikitin and A. I. Reznikov, Mol. Phys. **77**, 563 (1992).